[10] R. Pregla, "Method of lines for the analysis of multilayered gyrotropic waveguide structures," *IEE Proc. H,* vol. 140, no. 3, pp. 183–192, June 1993.
[11] M. Abramowitz and I. A. Stegun, *Handbook of Mathematical Functions with Formulas, Graphs, and Mathematical Tables.* New York: Dover.
[12] W. Pascher, "Full wave analysis of discontinuities in planar waveguides by the method of lines," in *Proc. URSI Int. Symp. Electromagnetic Theory,* Stockholm, Sweden, Aug. 1989, pp. 446–448.
[13] A. Dreher and R. Pregla, "Full-wave analysis of radiating planar resonators with the method of lines," *IEEE Trans. Microwave Theory Tech.*, vol. 41, no. 8, pp. 1363–1368, Aug. 1993.
[14] F. J. Schmückle and R. Pregla, "The method of lines for the analysis of planar waveguides with finite metallization thickness," *IEEE Trans. Microwave Theory Tech.*, vol. 39, no. 1, pp. 107–111, Jan. 1991.
[15] R. Pregla, "Higher order approximation for the difference operators in the method of lines," *IEEE Microwave Guided Wave Lett.*, vol. 5, no. 2, Feb. 1995.
[16] H. Diestel and S. B. Worm, "Analysis of hybrid field problems by the method of lines with nonequidistant discretization," *IEEE Trans. Microwave Theory Tech.*, vol. 32 , no. 6, pp. 633–638, June 1984.

Magnetic Frequency-Tunable Millimeter-Wave Filter Design Using Metallic Thin Films

Hoton How, Ta-Ming Fang, and Carmine Vittoria

***Abstract*— Frequency tunable millimeter wave filters are considered to be fabricated using metallic ferromagnetic thin films. Whereas conventional filters which include insulating ferrite materials utilize the phenomenon of ferromagnetic resonance (FMR), our design incorporates the phenomenon of ferromagnetic anti-resonance (FMAR). Our calculations indicate that in comparing the characteristics of the two types of filters the filter utilizing magnetic metal films is superior in terms of insertion loss and integrability with other planar millimeter wave devices. Design of band-pass filter can be realized in which the transmission frequency occurs at FMAR frequency with a frequency bandwidth equal to the FMAR linewidth.**

I. Introduction

In the past microwave/millimeter wave filters were inevitably designed in terms of varying the capacitive or inductive loading of the resonators. For the former case varactors are commonly used in which the frequency tuning range of the filter can be only a few percent of the transmission frequency [1]. For the latter case ferrite insulators are used which are usually in the form of polished spheres of single crystal yttrium iron garnet (YIG). The ferrite spheres are biased by a magnetic field and the transmission frequency is designed at ferromagnetic resonance (FMR) [2]. Both designs involving varactors and ferrite insulators are limited to relatively low-power applications.

We consider in this paper for the first time a new design in which metallic magnetic films are used instead of ferrites in order to improve the band-pass characteristics. Whereas conventional insulating ferrite materials utilize the phemomenon of ferromagnetic resonance (FMR), the use of magnetic metal films utilizes the phenomenon of ferromagnetic anti-resonance (FMAR). Normally metals more than a few μ thick are opaque to microwave radiation. However, it was predicted by Kaganov [3] (1959) and discovered by Heinrich and Meshcheryakov [4] (1969) that a ferromagnetic metal becomes relatively transparent to microwave radiation over a limit range of applied magnetic fields near the field strength corresponding to FMAR. At FMAR the effective permeability of the metal film is very small and, hence, the resultant microwave skin depth becomes anomalously large. Additional work on this subject may be found in [5]–[7].

Our filter design involves the fabrication of a composite microstrip line in which a thin magnetic metal film is inserted in the substrate layer of the microstrip line, which is connected to and lies parallel to the ground plane. The characteristic impedance of the microstrip line in the absence of the metal film is 50 Ω. A dc magnetic field is applied normal to the film plane. When the magnetic film is biased away from FMAR the magnetic metal film interferes strongly with wave propagation. The characteristic impedance of the line appears to be much smaller than 50 Ω. The signal is reflected when biased off-FMAR due to impedance mismatch. However, for biasing field at FMAR the skin depth within the magnetic metal becomes substantially greater than the film thickness. Consequently, at FMAR the impedance of the line changes to 50 Ω which matches the input signal feeder line. The band-pass transmission bandwidth is consequently the FMAR linewidth [5]–[7]. We have calculated the transmission properties of the filter based on the use of permalloy thin films. The calculations show the following characteristics: insertion loss is less than 0.2 dB, isolation larger than 10 dB, and frequency tunability extends from 30 to 120 GHz.

FMAR occurs for frequencies somewhat above FMR. At FMAR the rf magnetic moment, $\boldsymbol{m}$, is out-of-phase with the driving field, $\boldsymbol{h}$, so that [5]–[7]

$$\boldsymbol{b} = \boldsymbol{h} + 4\pi\boldsymbol{m} = 0. \tag{1}$$

For this condition the dynamic permeability, μ, is very small (limited by the value of magnetic relaxation) and the effective skin depth is large, being limited only by the magnetic damping. The condition of (1) combined with the magnetic equation of motion

$$\boldsymbol{M} = \gamma \boldsymbol{M} \times \boldsymbol{H} \tag{2}$$

where

$$\boldsymbol{H} = \boldsymbol{H}_0 + \boldsymbol{h}$$

readily leads to the condition for FMAR

$$\omega/\gamma = B_0 = H_{\text{in}} + 4\pi M_s \tag{3}$$

where H_{in} is the static internal magnetic field, γ the gyromagnetic ratio, and $4\pi M_s$ the saturation magnetization.

At FMAR the metal film is characterized by a small permeability value which results in very large skin depth when the metal film is exposed to rf excitations [5]–[7]. Therefore, the metal film appears to be transparent to the microwave millimeter wave transmission when it is biased at FMAR. The frequency bandwidth of transmission is roughly equal to the linewidth at FMAR [3]

$$\Delta H_{\text{FMAR}} = 0.3(4\pi M_s)[(\delta_s/d)(\Delta H/M_s)^{3/2}]^{1/2} \tag{4}$$

where d is the thickness of the metal film, δ_s the classical skin depth

$$\delta_s = c/(2\pi\sigma\omega)^{1/2}$$

c the speed of light in vacuum, σ the conductivity of the metal film, and ΔH is the linewidth at FMR given by

$$\Delta H = 2(\lambda/\gamma)(\omega/\gamma M_s). \tag{5}$$

Here λ denotes the Landau–Lifshitz damping parameter [6].

Manuscript received February 16, 1994; revised January 20, 1995. This work was supported by the Strategic Defense Initiative Office and managed and executed by the Defense Nuclear Agency (Contract DNA001-94-C-0076).

H. How and T.-M. Fang are with the Massachusetts Technological Laboratory, Belmont, MA 02178 USA.
C. Vittoria is with Northeastern University, Boston, MA 02115 USA.

IEEE Log Number 9412030.

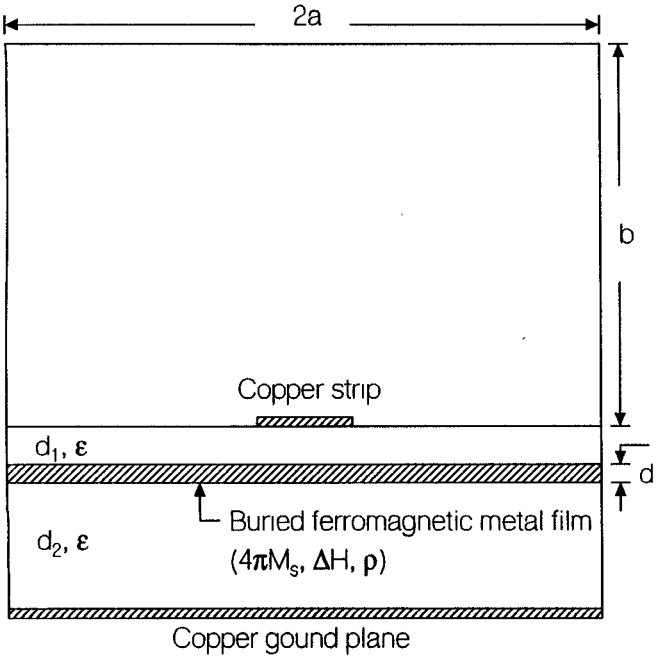

Fig. 1. Schematic drawing of the filter design incorporating magnetic thin film in a microstrip line.

II. Calculations

In the filter design considered by us a thin magnetic metal is inserted in the substrate layer of a microstrip transmission line which lies parallel to the ground plane, see Fig. 1. The metal film is characterized by thickness, d, saturation magnetization, $4\pi M_s$, FMR line width ΔH, and resistivity, $\rho = 1/\sigma$. The copper microstrip is of width w and the substrate thicknesses are denoted as d_1 and d_2, respectively, see Fig. 1. In the absence of metal film, i.e., $d = 0$, the characteristic impedance of microstrip is designed to be 50 Ω [8]. Therefore, when biased at FMAR the characteristic impedance of the composite microstrip line of Fig. 1 is roughly 50 Ω, since the metal film is almost invisible to the microwave propagation along the line. However, when biased off-FMAR the magnetic thin film becomes effectively the ground plane and the resultant transmission-line impedance can be much less than 50 Ω if d_1 is much smaller than d_2. The signal at the filter input is reflected due to impedance mismatch.

In the formulation we used a finite-difference calculational scheme in which the microstrip assembly is enclosed by finite (perfect) metal boundaries, $2a$ and b, respectively, see Fig. 1. We will let a and b go to infinity in the final answer to simulate an infinite composite microstrip line. The effective permeability of the metal film is [6]

$$\mu = \mu_1 + \mu_2^2/\mu_1 \tag{6}$$

where

$$\mu_1 = 1 + \frac{4\pi M_s H^*}{H^{*2} - f^2/\gamma^2}, \quad \mu_2 = \frac{4\pi M_s f/\gamma}{H^{*2} - f^2/\gamma^2} \tag{7}$$

$$H^* = H_{\text{in}} + j\alpha f/\gamma,$$

$$H_{\text{in}} = H_0 - 4\pi M_s,$$

and α is the Gilbert damping constant. The effective permittivity of the metal film is

$$\epsilon = 4\pi i\sigma/\omega.$$

Let the strip width be w and the four shielded planes be located at $x = -a$, $x = a$, $y = b$, and $y = -(d_1 + d + d_2)$. In the following we will use the (dynamic) gauge-fields in the calculations of the characteristic impedance, Z_o, and the propagation constant, k, for the microstrip line [9]. Denote z-axis to be along the microstrip line. Electric field, $\boldsymbol{E}$, and magnetic induction, $\boldsymbol{B}$, may be derived from a scalar potential, Φ, and a vector potential, $\boldsymbol{A}$, by the following equations

$$\boldsymbol{E} = -\underline{\nabla}\Phi - \partial\boldsymbol{A}/\partial t, \quad \boldsymbol{B} = \underline{\nabla} \times \boldsymbol{A}. \tag{8}$$

Under Lorentz gauge Φ and $\boldsymbol{A}$ are related by

$$\underline{\nabla} \cdot \boldsymbol{A} + \epsilon\mu\, \partial\Phi/\partial t = 0 \tag{9}$$

and Φ and $\boldsymbol{A}$ satisfy the following Helmholtz equations

$$(\nabla^2 - \epsilon\mu\, \partial^2/\partial t^2)\Phi = 0, \tag{10}$$

$$(\nabla^2 - \epsilon\mu\, \partial^2/\partial t^2)\boldsymbol{A} = 0. \tag{11}$$

Let the fields have the following dependence: $\exp[j(\omega t - kz)]$. For TM modes one may show below that $\boldsymbol{A}$ shall be parallel to the z-axis and from (10) and (11) one derives

$$\boldsymbol{A} = (\epsilon\mu\omega/k)\Phi\,\hat{z}, \tag{12}$$

$$\boldsymbol{E} = -\nabla_t\Phi + jk\,\hat{z}(1 - \epsilon\mu\omega^2/k^2)\Phi, \tag{13}$$

$$\boldsymbol{B} = (\epsilon\mu\omega/k)\hat{z} \times \nabla_t\Phi. \tag{14}$$

The advantages of adopting the above gauge-field expressions for the TM waves in the composite microstrip configuration are as follows. Firstly, the lowest mode in a microstrip line may be approximated as TM waves. In this case one has to solve a second-order Helmholtz equation, (10), in a two-dimensional geometry, Fig. 1. Secondly, since all of the shielded surfaces and the metal strip are parallel to the z-axis, the induced surface charges can be calculated from (13) as

$$\sigma_s = -\epsilon\partial\Phi/\partial n \tag{15}$$

where $\hat{n}$ denotes the unit direction normal to the surface. Equation (15) resembles exactly the static case in which Φ takes the place of a static potential.

Equation (10) can be solved for the composite microstrip line shown in Fig. 1 using finite difference method. The boundary conditions at the layer-layer interfaces are that Φ and $\epsilon\mu\partial\Phi/\partial y$ are continuous across the interfaces: $y = 0$, $y = -d_1$, and $y = -(d_1 + d)$. Perfect conductor boundary conditions, $\partial\Phi/\partial n = 0$, are assumed at the shielded metal surfaces: $x = -a$, $x = a$, $y = b$, and $y = -(d_1 + d + d_2)$. Here $\hat{n}$ denotes the unit direction normal to the shielded surfaces. Propagation constant k, which is a complex number in general, can be determined by imposing the zero-charge condition in which the total charges induce over all of the metal surfaces are zero

$$\int_{\sum} \hat{n} \cdot \nabla_t\Phi = 0 \tag{16}$$

where $\sum$ denotes all of the metal surfaces. The effective dielectric constant for the composite structure of the microstrip line, ϵ_r, can be calculated from the propagation constant k as

$$\epsilon_r = \omega(\epsilon_o\mu_o)^{1/2}/\text{Re}\,(k). \tag{17}$$

The characteristic impedance of the line, Z_o, is derived from ϵ_r and ϵ_{ro}, which are the capacitances per unit length of the line, as [8]

$$Z_o = \sqrt{\frac{\epsilon_o\mu_o}{\epsilon_r\epsilon_{ro}}} \tag{18}$$

where ϵ_{ro} represents the value of the capacitance per unit length when the layers are replaced by air. For the case of single-layer substrate, $d = 0$ and $\epsilon_1 = \epsilon_2$, calculations for ϵ_r and Z_o using the above gauge-field method give rise to exactly the same results as the conventional method for a microstrip line [9].

Let the above microstrip line of length L, which is connected to two 50 Ω feeder lines. Denote the characteristic impedance and wave propagation constant of the feeder lines by Z_1 and k_1, respectively. The reflection coefficient, R, at the input port and transmission coefficient, T, at the output port can be calculated to be

$$R = -Y(E - 1/E), \tag{19}$$

$$T = Y(X - 1/X)\exp(jk_1L) \tag{20}$$

where E, X, and Y are defined as

$$E = \exp(-jk_oL),$$

$$X = (Z_o - Z_1)/(Z_o + Z_1),$$

$$Y + [EX - (EX)^{-1}]^{-1}.$$

Scattering parameters, S_{11} and S_{21}, are therefore

$$S_{11} = 20\log_{10}|R|, \quad \text{and} \quad S_{21} = 20\log_{10}|T|. \tag{21}$$

III. Results

The transmission characteristics of the above line of length L have been calculated assuming 50 Ω air feeder lines. Fig. 2 shows the transmission curves as a function of frequency for various external biasing field strength, H_o. In Fig. 2 we have used the following parameters:

$$\epsilon = 5$$

$$d_1 = 0.05 \text{ mm}$$

$$d_2 = 0.5 \text{ mm}$$

$$d = 10\ \mu\text{m}$$

$$w = 0.885 \text{ mm}$$

$$L = 0.5 \text{ mm}$$

$$4\pi M_s = 10 \text{ kG (permalloy)}$$

$$\Delta H = 50 \text{ Oe (at 30 GHz)}$$

$$\rho = 4.68\ \mu\Omega \text{ cm (permalloy)}.$$

It is seen in Fig. 2 that the transmission occurs at FMAR frequency with a bandwidth roughly equal to the FMAR linewidth. The transmission frequency is tuned from 30 to 70 GHz with insertion loss less than 0.2 dB, isolation larger than 10 dB, and frequency bandwidth less than 2 GHz. In order to enhance isolation larger L and smaller d_1 values may be used.

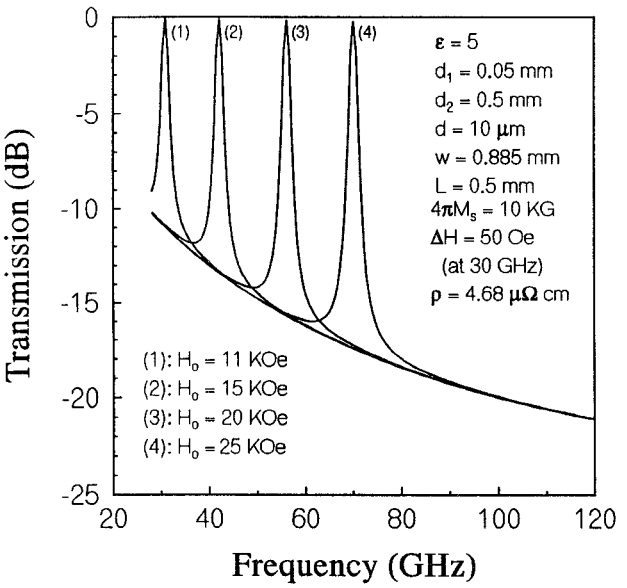

Fig. 2. Transmission characteristics of the filter biased at various magnetic fields.

IV. Conclusion

The insertion loss for a resonant-type filter is inevitably high, since at FMR energy dissipates as heat when the precessing motion of spins is damped by magnetic relaxation. Furthermore, the frequency tuning range of the filter is limited by the excitation of higher-order magnetostatic modes appearing as spurious transmission. Instead of utilizing ferromagnetic resonance phenomenon associated with a ferrite insulator we have considered in this paper the fabrication of nonresonant frequency-tunable band-pass filters using ferromagnetic metals which are biased at ferromagnetic anti-resonance (FMAR). Since the devices are biased off-resonance, the filters exhibit low insertion loss which can be applied under relatively higher power conditions. However, the calculated isolation exhibit lower values than that obtained from a resonant-type YIG filer [2]. In order to increase the frequency tuning range of the filter metal films other than permalloy with lower magnetization saturation values are preferred to be used. For example, cobalt alloyed magnetic thin films can have very small $4\pi M_s$ values. Of particular interest we propose the use of $Co_{74}Ge_6B1_5Si_5$ thin films, since they possess nearly zero magnetostriction coefficients and exhibit very small magnetization saturation values [10]. Our tunable filter design provides great advantage over the traditional YIG filters in terms of tuning frequency range, response time, and compatibility with other planar microwave circuits. Frequency tunable filters are desirable for radar transmitter-receiver module applications in order to eliminate receiver images as well as to increase amplifier efficiency.

References

[1] J. Uher and W. J. R. Hoefer, "Tunable microwave and millimeter-wave band-pass filters," *IEEE Trans. Microwave Theory Tech.*, vol. 39, p. 643, 1991.
[2] R. Roeschmann, "YIG filters," *Phillips Tech. Res.*, vol. 32, p. 322, 1971.
[3] M. Kagonov, *Fiz. Met. Metalloved,* vol. 7, p. 287, 1959.
[4] B. Heinrich and Machcheryakov, *JETP Lett.*, vol. 9, p. 378, 1969.
[5] J. M. Rudd, J. F. Cochran, K. B. Urquhart, K. Mytle, and Heinrich, "Ferromagnetic antiresonance transmission through pure iron at 73 GHz," *J. Appl. Phys.*, vol. 63, p. 3811, 1988.
[6] P. Lubitz and C. Vittoria, "Remarks on antiresonance in ferromagnetic metals," in *AIP Conf. Proc.*, vol. 24, 1975, p. 507.
[7] J. F. Cochran, B. Heinrich, and G. Dewar, "Ferromagnetic antiresonance transition through supermalloy at 24 GHz," *Can. J. Phys.*, vol. 55, p. 787, 1977.

[8] T. C. Edwards, *Foundations for Microstrip Circuit Design.* New York: Wiley, 1987.
[9] H. How and C. Vittoria, "Design of drop-in microstrip circulator," *IEEE Trans. Microwave Theory Tech.,* submitted, 1993.
[10] V. G. Harris, S. A. Oliver, W. B. Nowak, and C. Vittoria, "Magnetic and microwave resonance properties of ion beam sputtered amorphous $Fe_xCo_{80-x}B_{15}Si_{15}$ films," *J. Appl. Phys.,* vol. 67, p. 5571, 1990.

Quick Computation of $[C]$, $[L]$, $[G]$, and $[R]$ Matrices of Multiconductor and Multilayered Transmission Systems

Gonzalo Plaza, Francisco Mesa, and Manuel Horno

***Abstract*—This paper presents a general scheme to compute the four characteristic matrices, $[C]$, $[G]$, $[L]$ and $[R]$, of a multilayered and multiconductor transmission line with arbitrary cross section conductors under quasi-TEM approach and strong skin effect regime. The conductors are modeled as a set of infinitesimally thin strips following the M-strip model. An spectral domain approach (SDA) has been employed, paying special attention to the efficient computation of the spectral tails. Conductor losses are considered via the incremental inductance rule extended to the multiconductor case.**

I. Introduction

The computation of the TEM (or quasi-TEM) parameters of multiconductor transmission lines having arbitrary cross section conductors embedded in a layered medium is basic for the design and analysis of a variety of technological problems ranging from microwave integrated/printed circuits to high speed interconnects. Several methods have been gradually reported in the literature to compute these parameters, although general treatments have been only provided recently. Some of these general methods, following different techniques, have been reported in [1]–[3] and [4]. In [5] and [6] the authors proposed and developed the M-strips model to analyze arbitrary cross section perfect conductors in a multilayered medium without restriction on those dielectric and magnetic properties compatible with the quasi-TEM approach.

In the present work, we present a new mixed spectral/spatial domain approach to compute the characteristic matrices of transmission lines with arbitrarily cross section conductors (in laterally open environment) using the M-strips model. We have attained a good numerical efficiency by combining the complex images technique [7] with a nontrivial extension of the guide lines suggested in [8] to evaluate the required inner products and convolutions and the use of recurrence relationships [6]. We have also incorporated the study of conductor losses under strong skin effect regime by computing the resistance matrix via an extension of the incremental inductance rule of Wheeler to a multiconductor line [9].

II. Analysis

Following the M-strip model [5], each original conductor with arbitrary cross section is modeled as a set of infinitesimally thin strips at the same potential and circumscribed to the contour of the original conductor. The corresponding spectral integral equation is solved via the Galerkin's method (using as spatial basis function the Chebyshev's polynomials weighed by the Maxwell's distribution). The spectral integrals appearing in the Galerkin's matrix show the following form

$$\Gamma_{ipn}^{jqm} = \int_{-\infty}^{+\infty} J_n\left(\frac{w_p k_x}{2}\right) G_{ij}(k_x) J_m\left(\frac{w_q k_x}{2}\right) e^{jk_x s}\, dk_x \tag{1}$$

where the subscripts p and q are used to number the strips in the model, $w_{p(q)}$ is the width of each strip; $s = c_q - c_p$ with $c_{p(q)}$ being the abscisa of their centers; J_n is the Bessel function of order n and $G_{ij}(k_x)$ is the spectral Green's function for a source line at the jth metallizated level (where qth strip is placed) and field points at the ith level (where pth strip is placed).

Since the numerical efficiency of the SDA is strongly determined by the fast and accurate computation of the spectral integrals, we have paid an especial attention to accelerate its computation because we face to a very slow convergence caused by extremely close strips. We have used the asymptotic integration scheme shown in [6], where the asymptotic behavior of the spectral Green's function, G_{ij}^{∞}, is now expressed following the complex images technique [7]

$$G_{ij}^{\infty}(k_x) = \sum_{n=1}^{N} A_n^{ij} \frac{\exp(\Omega_n^{ij} k_x)}{k_x}. \tag{2}$$

Expansion (2) provides a very good fitting of the spectral Green's function and thus the integrals involving $G - G^{\infty}$ converge quickly. In consequence, the efficiency of the proposed integration technique lies basically in the computation of the integral tails. The generic form, except for constants, of these integral tails is

$$I_n^m = \int_u^{\infty} J_n(ak_x) J_m(bk_x) \frac{e^{(-\beta+jd)k_x}}{k_x}\, dk_x \tag{3}$$

where u is a suitable value to start using the asymptotic behavior; a and b are the semiwidths of the strips; $\beta = -\mathrm{Re}(\Omega)$ and $d = s + \mathrm{Im}(\Omega)$ (Ω stands for any of the complex exponents in (2)). The new distance, d, can be seen as a modified distance between the centers of the strips in the integrals tails.

The integral tails (3) are computed by reversing them to the spatial domain via Parseval's theorem. The use of Parseval's theorem requires a previous extension of the tails from $-\infty$ to $+\infty$. This extension is readily made by multiplying the integrand in (3) by the step function $H(k_x - u)$ and so, the following spatial domain integral is obtained

$$I_n^m = \frac{j^n(-j)^m}{\pi^2} \int_{-1}^{1} \frac{T_n(\gamma)}{\sqrt{1-\gamma^2}} \cdot \left[\int_{-1}^{1} \frac{T_m(\alpha)}{\sqrt{1-\alpha^2}} E_1(u\zeta)\, d\alpha\right] d\gamma \tag{4}$$

where $\zeta = \beta + j(a\gamma - b\alpha - d)$. α and γ appear after changing the integration variable (both in the convolution integral in α- and the inner product integral in γ-) into the interval $(-1, 1)$ and $E_1(u\zeta)$ stands for the exponential integral function, which can be expanded as shown in [10]. The convolution product in expression (4) might be regarded as a complex *potential* originated by a strip of width $2b$ (*source-strip*) over a second strip of width $2a$ (*observer-strip*) placed at a height β above the first one, and with its center laterally separated a distance d. We will express ourselves in these terms to simplify the descriptions in the below analysis.

Manuscript received September 26, 1994; revised January 20, 1995. This work was supported by the DGICYT, Spain TIC91-1018.

The authors are with the Microwave Group, Department of Electronics and Electromagnetism, University of Seville, 41012 Seville, Spain.

IEEE Log Number 9412034.